ACCOUNTS
of chemical research

# Ligands for Mapping $\alpha_v\beta_3$-Integrin Expression in Vivo

MARGRET SCHOTTELIUS,[†,§] BURKHARDT LAUFER,[‡,§]
HORST KESSLER,[‡] AND HANS-JÜRGEN WESTER[*,†]

*[†]Nuklearmedizinische Klinik und Poliklinik, Klinikum rechts der Isar, Technische Universität München, 81675 München, Germany, [‡]Center for Integrated Protein Science at the Technische Universität München, Department Chemie, 85747 Garching, Germany*

RECEIVED ON OCTOBER 21, 2008



## CONSPECTUS

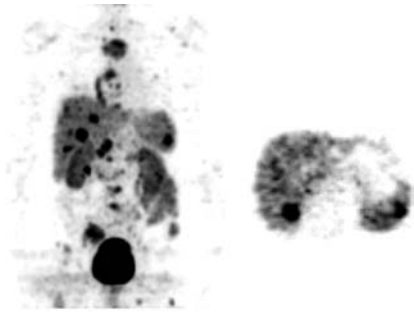

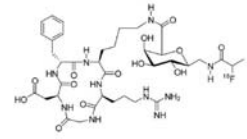

[$^{18}$F]GalactRGD

The $\alpha_v\beta_3$- and $\alpha_5\beta_1$-integrins play a key role in angiogenesis, the formation of new vessels in tissues that lack them. By serving as receptors for a variety of extracellular matrix proteins containing an arginine-glycine-aspartic acid (RGD) sequence, these integrins mediate migration of endothelial cells into the basement membrane and regulate their growth, survival, and differentiation. Besides being involved in angiogenesis, the $\alpha_v\beta_3$-integrin is also presented on tumor cells of various origin, where it is involved in the processes that govern metastasis.

Because the $\alpha_v\beta_3$-integrin is an attractive target for cancer treatment, high-affinity ligands containing the RGD sequence, for example, cydic pentapeptides, have been developed. They inhibit angiogenesis, induce endothelial apoptosis, decrease tumor growth, and reduce invasiveness and spread of metastasis. This development finally resulted in *cyclo*(RGDf(*NMe*)V) (cilengitide), which is a drug for the treatment of glioblastoma (currently in phase III clinical trials).

With the growing focus on individualized medicine, clinicians would like to be able to assess the severity of the disease and monitor therapy for each patient. Such measurements would be based on a noninvasive visualization and quantification the $\alpha_v\beta_3$-integrin expression levels before, during, and after antiangiogenic therapy. A wide spectrum of in vivo imaging probes for the nuclear imaging modalities positron emission tomography (PET) and single-photon emission computed tomography (SPECT), for optical imaging, and for magnetic resonance imaging (MRI) have been developed with these goals in mind. In this Account, we describe the synthesis and preclinical and clinical assessments of dedicated targeting probes. These molecules ideally accumulate selectively and in high concentrations in $\alpha_v\beta_3$-integrin-expressing tissues, have low uptake and retention in nontarget tissues, and are highly stable against in vivo degradation.

[$^{123}$I]*cyclo*(RGDyV) was the first radiolabeled "imaging analogue" of cilengitide that we evaluated preclinically in detail. Subsequent studies focused on *cyclo*(RGDfK) and *cyclo*(RGDyK), which allowed conjugation with various signaling moieties, such as prosthetic groups, bifunctional chelators (DTPA, DOTA, NOTA, TETA, and TE2A for labeling with $^{111}$In or $^{177}$Lu for SPECT and $^{86}$Y, $^{68}$Ga, or $^{64}$Cu for PET), or fluorescent dyes (Cy5.5, cypate). Furthermore, pharmacokinetic modifiers such as carbohydrates, charged amino acids, or PEG analogues were coupled to the peptide core without significantly affecting the binding affinity. Finally, dimers, tetramers, octamers, and polymers and decorated quantum dots with several dozens of peptide units were constructed and investigated. Some of these multimers demonstrated significantly improved affinity (avidity) and targeting efficiency in vivo.

Besides peptidic $\alpha_v\beta_3$-integrin ligands, researchers have investigated radiolabeled antibodies such as Abegrin and used molecular modeling to design small peptidomimetics with improved activity, in vivo stability, and subtype selectivity (e.g., $^{111}$In-TA138). Furthermore, there is an increasing interest in nanoparticles such as nanotubes, quantum dots, or paramagnetic particles coated with cyclic RGD analogues as targeting agents. [$^{18}$F]Galacto-RGD, a glycosylated *cyclo*(RGDfK) analogue, was the first such substance applied in patients and has been successfully assessed in more than 100 patients so far.

Because of modification with carbohydrates, rapid renal excretion, and inherently low background activity in most regions of the body, imaging of $\alpha_v\beta_3$ expression with high tumor/background ratios and high specificity is possible. Other $^{18}$F-labeled RGD analogues recently developed by Siemens and GE Healthcare have entered clinical trials.

Published on the Web 06/02/2009 www.pubs.acs.org/acr
10.1021/ar800243b CCC: $71.50 

## Introduction

Angiogenesis, the process of formation of new vessels in avascular tissue, plays a key role in a variety of processes such as embryogenesis, tissue remodeling, the female reproductive cycle, and wound healing and is also upregulated in a variety of deseases, for example, rheumatoid arthritis, psoriasis, restenosis, diabetic retinopathy, and tumor growth, as well as tumor metastasis. The angiogenic process depends on vascular endothelial cell migration and invasion, which are regulated by cell adhesion receptors such as integrins.[1,2] Their function ranges from mediating migration of endothelial cells into the basement membrane to regulation of endothelial cell growth, survival, and differentiation during angiogenesis.[3]

The $\alpha_v\beta_3$- and $\alpha_5\beta_1$-integrins serve as receptors for a variety of extracellular matrix proteins with the exposed arginine-glycine-aspartic acid (RGD) sequence, for example, vitronectin or fibronectin. Since the $\alpha_v\beta_3$-integrin is expressed on the tumor cells of certain tumor types (melanoma, glioblastoma, ovarian, and breast cancer), it represents an attractive target for cancer therapy.[4] High-affinity $\alpha_v\beta_3$-integrin ligands based on RGD-peptides inhibit angiogenesis, induce endothelial apoptosis, decrease tumor growth and reduce invasiveness and spread of metastasis.

A wide spectrum of probes for various imaging modalities, ranging from nuclear imaging (SPECT (single photon emission computed tomography) and PET (positron emission tomography)) over magnetic resonance (MR) and ultrasound (US) to optical imaging methods (e.g., FMT (fluorescence mediated tomography)), have been investigated to noninvasively visualize the $\alpha_v\beta_3$-integrin expression status before, during, and after antiangiogenic therapy. These approaches require dedicated and chemically modified $\alpha_v\beta_3$-integrin targeting probes, which optimally fulfill three requirements: high selective and specific uptake, low accumulation and retention in nontarget tissues, and high in vivo stability.

Development of such targeting probes therefore focuses on the choice of an optimal targeting moiety and the pharmacokinetic optimization after modification with a suitable signal unit, that is, a radionuclide (SPECT/PET), a fluorescent dye (FMT), or a contrast agent (US, MR).

For peptide receptor mapping, SPECT and PET have the highest clinical impact, which has prompted intense efforts in the development of $\alpha_v\beta_3$-integrin targeted radiopharmaceuticals.[5] This class of tracers therefore serves best to illustrate the various aspects of probe development. Thus, this Account will focus on the comparative assessment of radiolabeled $\alpha_v\beta_3$-integrin probes.

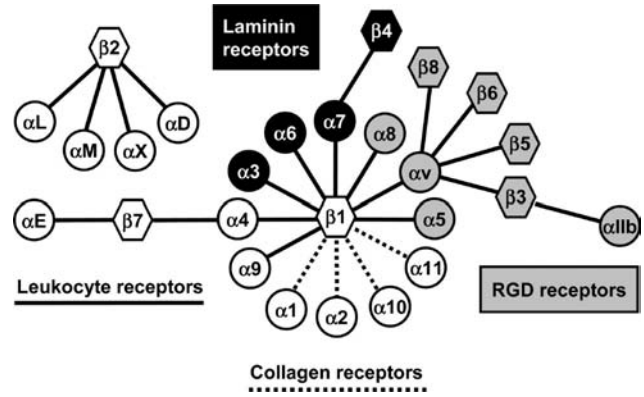


**FIGURE 1.** The integrin family: RGD receptors, laminin receptors, leukocyte receptors, and collagen receptors.

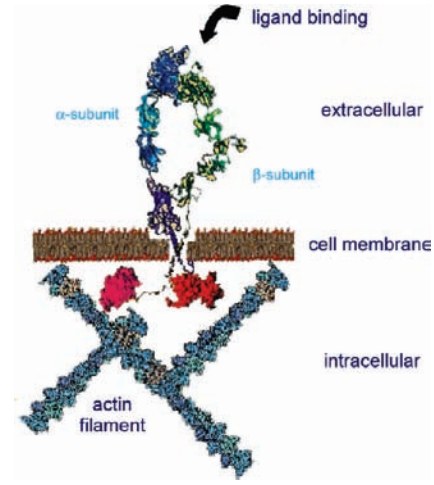


**FIGURE 2.** An integrin receptor in the fully extended conformation.

## INTEGRINS AND THEIR LIGANDS

**Integrins.** Integrins constitute a family of heterodimeric transmembrane cell adhesion receptors (Figure 1), which connect cells to proteins of the extracellular matrix. Until now, 18 α and 8 $\beta$ subunits have been identified. They form 24 heterodimers, each with distinct ligand binding properties, able to perform inside-out and outside-in signaling.[4,6] Each of the α and $\beta$ subunits is a type I membrane glycoprotein consisting of a large extracellular domain, a transmembrane helix, and a short cytoplasmic tail (Figure 2).[7] Integrins are often detected in clusters on cell surfaces, which is, in some cases, required for their ligand-binding ability.[8]

The RGD sequence has been identified as an essential binding motif for seven out of the 24 integrin receptors, for example, $\alpha_v\beta_3$ and $\alpha_5\beta_1$. This has stimulated ongoing research to define other small peptidic integrin-binding sequences.[9,10]

**Integrin Ligands.** The discovery of the RGD sequence as the essential binding motif was the starting point for the rapid development of a variety of small-molecule $\alpha_v\beta_3$-integrin antagonists with successively improving ligand characteris-

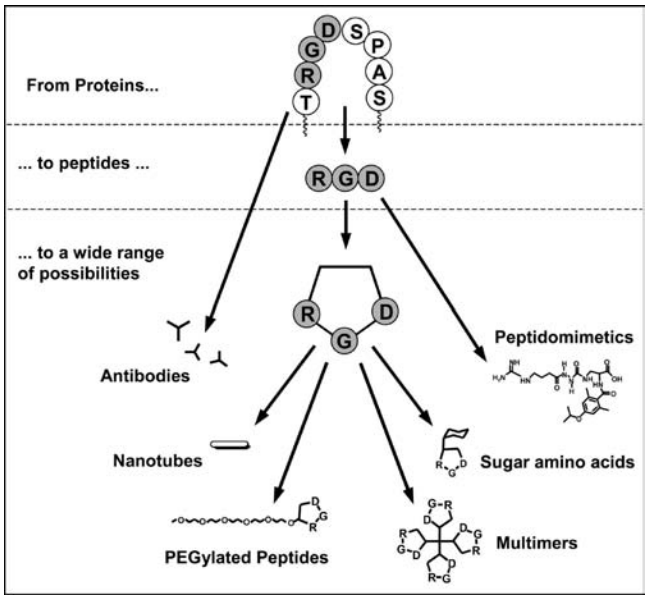


**FIGURE 3.** Evolution of RGD-containing compounds.

tics and suitable in vivo characteristics for antiangiogenic therapy (Figure 3).

First-generation linear peptides containing the RGD sequence or disulfide bridged cyclic peptides such as RGD-4C suffer from low subtype selectivity, from low metabolic stability, or from both.[11,12] High selectivity ($\alpha_v\beta_3 \gg \alpha_{IIb}\beta_3$), strongly enhanced activity, and sufficient metabolic stability have been observed for the cyclic pentapeptide *cyclo*(RGDfV), developed by a screening for the best spatial orientation of the RGD peptide sequence.[13] Additional optimization via *N*-methylation finally resulted in the cyclic peptide *cyclo*(RGDf(*NMe*)V), which is applied as a drug for the treatment of glioblastoma (cilengitide, clinical phase III).[14] This peptide shows subnanomolar $\alpha_v\beta_3$-affinity and low nanomolar $\alpha_5\beta_1$- and $\alpha_v\beta_5$-affinity. These three integrins are all involved in angiogenesis; selectivity toward the platelet integrin $\alpha_{IIb}\beta_3$ is high.

Unfortunately, except facile radioiodination after substitution of D-phenylalanine by D-tyrosine in *cyclo*(RGDfV), these cyclopeptides do not possess functionalities that allow efficient conjugation of alternative signaling units. Thus, [$^{123}$I]*cyclo*(RGDyV) was the first radiolabeled $\alpha_v\beta_3$-ligand evaluated in vivo.[15] Substitution of valine by lysine allowed conjugation with prosthetic groups, chelators, and dyes without significantly affecting binding affinity.[16] Use of the *cyclo*-(RGDf/yK) core furthermore facilitated optimization of pharmacokinetics via attachment of pharmacokinetic modifiers (e.g., carbohydrates,[17,18] charged amino acids,[16] PEG analogues[19,20]) or improved binding characteristics (avidity) via multimerization.[21,22] Besides peptidic $\alpha_v\beta_3$-integrin ligands, radiolabeled antibodies have been investigated in the context of immunotherapy of cancers to characterize the pharmacokinetics of the parent antibodies,[23] and molecular modeling has been exploited to design peptidomimetics with improved activity, in vivo stability, and subtype selectivity. For example, the availability of the X-ray structure of $\alpha_v\beta_3$ in complex with cilengitide[24] led the route toward a homology model of $\alpha_5\beta_1$,[25] allowing the rational design of peptidomimetic integrin ligands with significantly improved subtype specificity.[26,27]

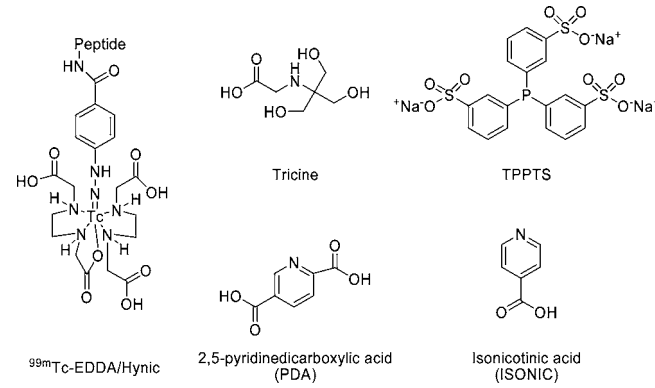


**FIGURE 4.** The $^{99m}$Tc(Hynic)(EDDA) complex and other coligands.

Furthermore, the use of nanoparticles such as nanotubes,[28] quantum dots,[29] or paramagnetic particles[30] coated with cyclic RGD analogues as targeting units is gaining more and more interest.[31]

In summary, a variety of $\alpha_v\beta_3$-targeted lead structures have evolved, and a multitude of labeling and optimization strategies are available for the development of suitable imaging agents.

## Integrin Ligands for in Vivo Imaging

**Nuclear Probes. $^{99m}$Tc-Labeled Compounds.** Of all clinically relevant radionuclides, $^{99m}$Tc-labeling requires the most fundamental structural changes, often leading to radioconjugates with unpredictable characteristics.

The earliest examples of $^{99m}$Tc-labeled $\alpha_v\beta_3$-integrin targeted compounds are the linear peptide G-RGD-SPC,[32] as well as αP2 (RGD-SC-RGD-SY),[33] using the cysteine side chain for complexation of $^{99m}$Tc. Evaluation of the latter peptide in patients with metastatic melanoma yielded low tumor/background ratios and poor imaging quality.

Much more stable complexation of $^{99m}$Tc has been achieved by using small peptides with several donor groups as chelators, for example, the DKCK sequence of DKCK-*cyclo*-(RGDfK).[34] This compound showed specific uptake in vivo but also high renal accumulation and low metabolic stability. Recently, an RGD-4C-functionalized HPMA polymer was labeled with $^{99m}$Tc via a MA-GG-DPK-chelator. Due to its long

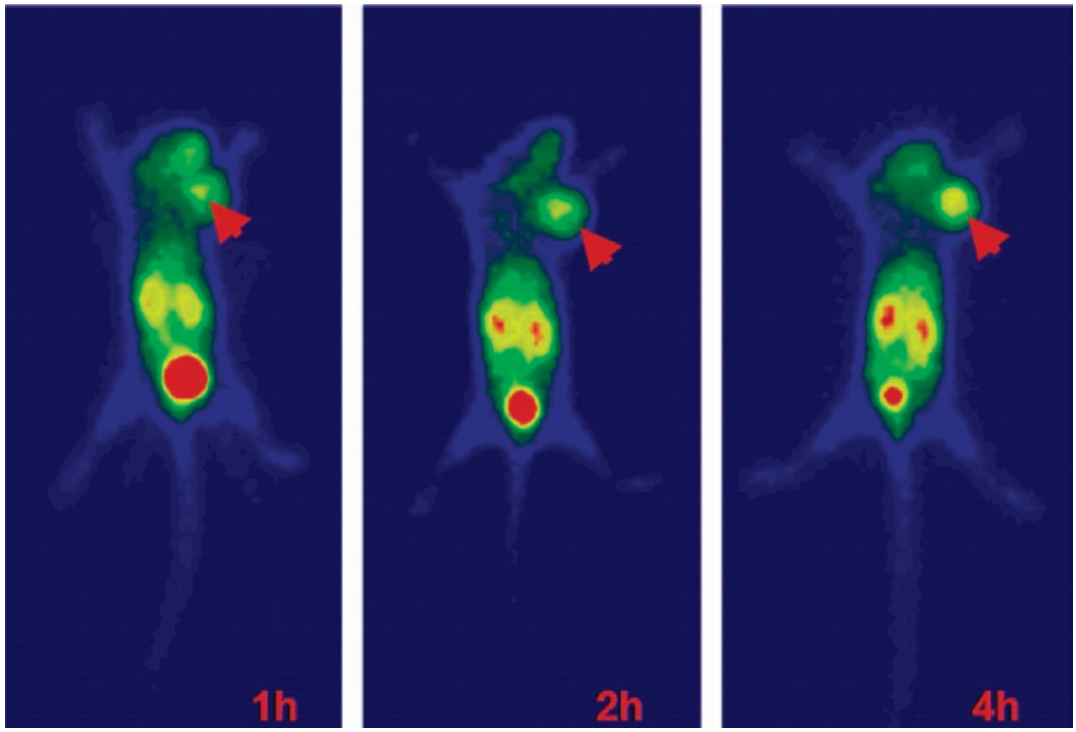


**FIGURE 5.** SPECT images of tumor-bearing mice 1, 2, and 4 h p.i. of ~15 MBq of $^{99m}$Tc(HYNIC-E{E[*cyclo*(RGDfK)]$_2$}$_2$)(tricine)(TPPTS). Reproduced from ref 40. Copyright 2007 American Chemical Society.



plasma half-life, tumor/background ratios suitable for imaging were reached as late as 24−72 h postinjection.

$^{99m}$Tc-labeling of the RGD-4C-derived analogue $^{99m}$Tc-NC100692,[12] which has a PEGylated C-terminus, was achieved via a diamine−dioxime chelator (see Figure 15). This compound shows efficient $\alpha_v\beta_3$-integrin targeting and is currently being evaluated in a clinical trial.[35]

The most frequently applied complexation chemistry for $^{99m}$Tc employs hydrazinonicotinic acid (HYNIC)-coupled precursor molecules and various coligands, which have significant impact on the in vivo performance of $^{99m}$Tc-HYNIC-labeled biomolecules.[36]

Among the HYNIC-conjugated $\alpha_v\beta_3$-integrin ligands, the dimeric HYNIC-E[*cyclo*(RGDfK)]$_2$ has been most extensively studied and shows a 10-fold increased receptor affinity compared with the monomeric analogue, which is reflected in an increased tumor accumulation and retention in vivo.[37] Both variation of the coligand (trisodium triphenylphosphine-3,3′,3″-trisulfonate (TPPTS) versus 2,5-pyridinedicarboxylic acid (PDA); Figure 4), and alternative introduction of an anionic linker between HYNIC and the peptide core in $^{99m}$Tc(HYNIC-E[*cyclo*(RGDfK)]$_2$)(tricine)(TPPTS) led to markedly increased tumor/kidney and tumor/liver ratios.[38,39] Enhanced $\alpha_v\beta_3$-integrin-mediated tumor uptake was also observed for tetrameric $^{99m}$Tc(HYNIC-E{E[*cyclo*(RGDfK)]$_2$}$_2$)(tricine)(TPPTS), while

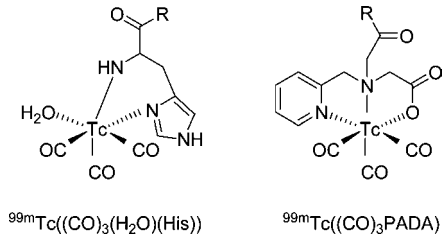


$^{99m}$Tc((CO)$_3$(H$_2$O)(His)) $^{99m}$Tc((CO)$_3$PADA)

**FIGURE 6.** Structures of the bidentate $^{99m}$Tc(CO)$_3$(H$_2$O)His complex and the tridentate PADA complex.

activity concentrations in blood and liver remained unchanged (Figure 5). Renal acitivity levels, however, also increased.[40]

Due to the availability of a kit formulation (IsoLink, Mallinckrodt), another $^{99m}$Tc-labeling strategy has gained considerable impact. Buffered pertechnetate eluted from the $^{99}$Mo/$^{99m}$Tc-radionuclide generator is reduced to the [$^{99m}$Tc(CO)$_3$(H$_2$O)$_3$]$^+$ aqua ion by sodium boranocarbonate and subsequently complexed with bidentate (e.g., histidine) or tridentate (e.g., *N*,*N*-picolylamine diacetic acid (PADA)) chelators (Figure 6).

In a first study, linear and cyclic $^{99m}$Tc-RGDfK-His and $^{99m}$Tc-RGDfK-PADA analogues exhibited considerable hepatic and intestinal accumulation, challenging their applicability for in vivo imaging studies.[41] Recently, four *cyclo*(RGDfK) moieties were grafted to a cyclic octapeptide (RAFT-RGD) and labeled with [$^{99m}$Tc(CO)$_3$(H$_2$O)$_3$]$^+$ via histidine.[22] Although this tetramer showed increased tumor accumulation, tumor/organ ratios

were <1 for almost all organs. Another attempt to improve pharmacokinetic properties of $^{99m}Tc(CO)_3$-labeled RGD analogues resulted in an Asp-glucosamino-derivative of *cyclo*-(RGDfK) using *N*-bis-carboxymethylglycine as chelator.[42] Again, uptake in liver, intestines, and kidney was higher than tumor uptake.

Generally, $^{99m}Tc(CO)_3$-labeled peptides show protein binding and hepatobiliary clearance. This has also been illustrated by a comparative study involving *cyclo*(RGDyK)-analogues labeled with $^{99m}Tc$ via four different strategies, which showed fundamentally different pharmacokinetic profiles.[43] Therefore, care must be taken in choosing the appropriate $^{99m}Tc$-labeling strategy. Subsequent optimization with respect to binding affinity and excretion profile, as exemplified by $^{99m}Tc$(HYNIC-E[*cyclo*(RGDfK)]$_2$) (see above), seems unavoidable.

**Radiometalated Compounds.** For radiometalation of $\alpha_v\beta_3$-integrin ligands, chelators such as DTPA (diethylenetriaminepentaacetic acid) or DOTA (1,4,7,10-tetraazacyclododecane-1,4,7,10-tetraacetic acid), both of which form complexes with a variety of clinically relevant radiometals ($^{111}In$ (SPECT), $^{177}Lu$ (pretherapy dosimetry); $^{68}Ga$, $^{64}Cu$, $^{86}Y$ (PET)) have been conjugated to RGD peptides (Figure 7).

As described for the $^{99m}Tc$-labeled analogues, initial studies were conducted using DTPA- and DOTA-*cyclo*(RGDf/yK) derivatives, which were then further optimized using various strategies.[44,45]

In a recent study, *cyclo*(RGDfK(DOTA)), labeled with $^{111}In$ and $^{68}Ga$, was evaluated in M21-melanoma bearing mice.[46] The $^{68}Ga$-labeled analogue showed higher activity concentrations in all organs compared with [$^{111}$In]DOTA-RGD, especially in blood and tumor. This resulted in slightly increased tumor/organ ratios for [$^{68}$Ga]DOTA-RGD despite high plasma protein binding. This example highlights the impact of radionuclide chelation properties on the biodistribution of otherwise identical tracer molecules.

The choice of the binding sequence, that is, *cyclo*(RGDyK) vs *cyclo*(RGDfK) also has substantial influence on ligand pharmacokinetics. In vivo comparison of two dimers, [$^{64}$Cu]DOTA−E[*cyclo*(RGDfK)]$_2$ and [$^{64}$Cu]DOTA−E[*cyclo*(RGDyK)]$_2$, showed significantly higher tumor accumulation of the D-tyrosine derivative compared with the D-phenylalanine analogue, along with a decreased liver uptake.[47]

Pharmacokinetic modifiers such as additional charged amino acids or large hydrophilic polymers have been introduced to reduce nonspecific tracer accumulation. In the case of dimeric [$^{111}$In]DTPA−E−E[*cyclo*(RGDfK)]$_2$, the glutamic acid spacers lead to significantly increased tumor/kidney and tumor/liver ratios without reducing tumor uptake,[48] and in the case of monomeric [$^{64}$Cu]DOTA-PEG(3400)−*cyclo*(RGDyK), modification with the PEG polymer (3400 Da) occasioned a decrease in hepatic and intestinal tracer accumulation without affecting tumor uptake.[19]

As described, multimerization of *cyclo*(RGDf/yK) units may be used as a tool to enhance receptor affinity and avidity. For example, tetrameric [$^{64}$Cu]DOTA−E{E[*cyclo*(RGDyK)]$_2$}$_2$ exhibits a 3-fold increased receptor affinity compared with the corresponding dimer and a doubling of tumor accumulation, accompanied by an increased activity accumulation in the excretion organs.[49] This trend is further continued in the transition from the tetrameric to the octameric compound.[50]

The same has been observed in studies with corresponding [$^{111}$In]DOTA and [$^{68}$Ga]NOTA analogues.[51,52] Whether this challenges the concept of multimerization beyond dimerization or simply reflects increased specific binding to other integrin subtypes has not been evaluated in detail so far.

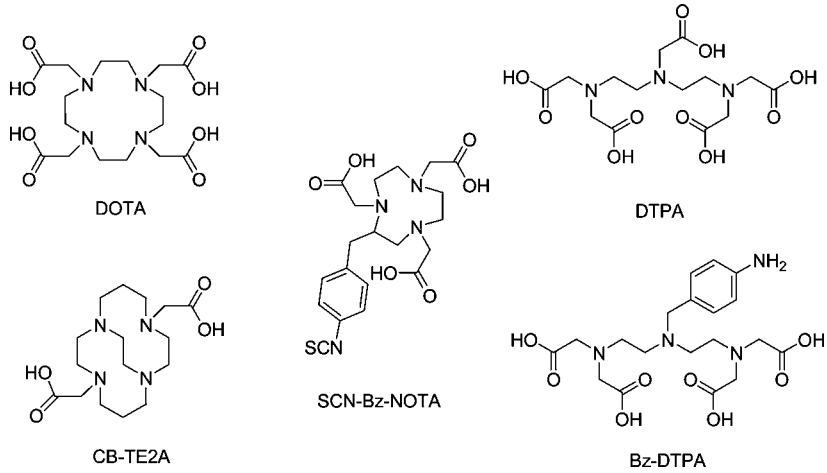


**FIGURE 7.** Bifunctional radiometal chelating systems.

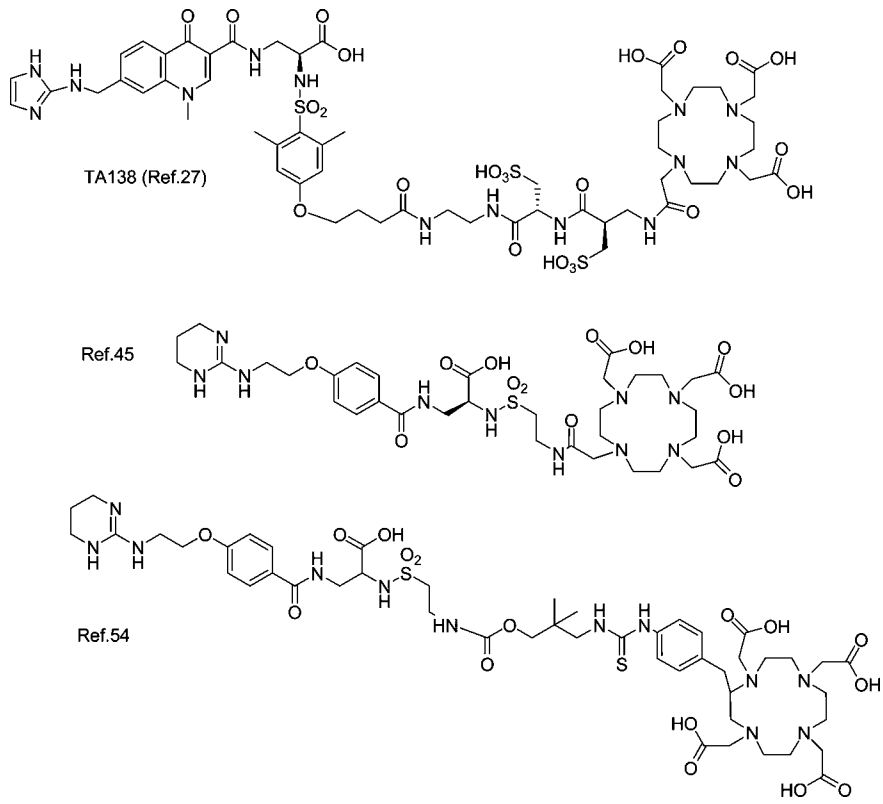


**FIGURE 8.** Structures of $^{111}$In-labeled peptidomimetics.

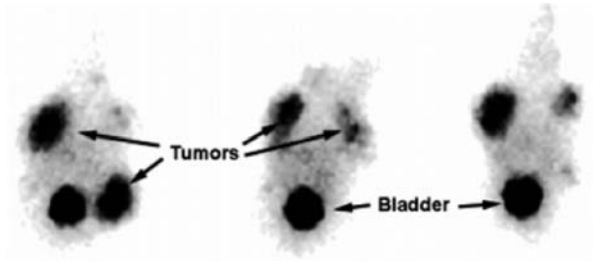


**FIGURE 9.** Scintigraphic images of $^{111}$In-TA138 (2 h p.i. of ~50 $\mu$Ci/mouse) in a c-neu oncomouse mammary adenocarcinoma model.[34]

Especially in the case of $^{64}$Cu-labeled compounds, the choice of the chelator may influence the biodistribution pattern. It is well-known, that DOTA and TETA complexes of $^{64}$Cu are susceptible to in vivo transchelation in the liver, leading to hepatic activity accumulation and retention. Cross-bridged chelators such as CB-TE2A form more stable $^{64}$Cu complexes, leading to decreased liver retention of [$^{64}$Cu]CB-TE2A–*cyclo*(RGDyK) compared with the DOTA derivative.[53]

Besides radiometalated RGD peptides, $^{111}$In-labeled small-molecule ligands have also been described (Figure 8).[27,45,54]

Among these, $^{111}$In-TA138 showed the most favorable pharmacokinetics and excellent imaging quality as early as 2 h postinjection (Figure 9).

Furthermore, Abegrin, a humanized mAb against human $\alpha_v\beta_3$-integrin, which is currently being investigated in clinical trials for cancer therapy, has been labeled with $^{64}$Cu and evaluated.[23] The $^{64}$Cu-DOTA conjugate seems to be well suited for characterization of the pharmacokinetics, tumor targeting efficiency, dose estimation, and suitable dose interval of Abegrin.

**Radiohalogenated Compounds.** Radioiodinated *cyclo*-(RGDyV) and *cyclo*(RGDfY) were the first radiolabeled $\alpha_v\beta_3$-ligands for noninvasive investigation of angiogenesis in vivo.[15] To reduce unspecific binding of [$^{125}$I]*cyclo*(RGDyV), the more hydrophilic [$^{123}$I]gluco-RGD, a *cyclo*(RGDyK) analogue derivatized with a sugar–amino acid was developed, resulting in superior imaging of $\alpha_v\beta_3$-expression in vivo.[17]

Since PET is the imaging methodology of choice, an analogous $^{18}$F-labeled compound, [$^{18}$F]galacto-RGD was developed.[18] This derivative shows pharmacokinetics comparable to [$^{123}$I]gluco-RGD but increased tumor uptake, yielding high-contrast PET images. Consequently, [$^{18}$F]galacto-RGD has been successfully applied for clinical imaging of $\alpha_v\beta_3$-integrin expression.

Other monomeric $^{18}$F-labeled RGD-peptides have been synthesized using direct radiofluorination,[55] acylation with succinimidyl-4-[$^{18}$F]fluorobenzoate[56] or hydrazone formation between 4-[$^{18}$F]fluorobenzaldehyde and HYNIC-*cyclo*(RGDyK) (Figure 10).[57] None, however, show a comparably favorable biodistribution pattern as [$^{18}$F]galacto-RGD.

Significant improvement was achieved by developing multimeric *cyclo*(RGDfE) analogues, which were radiofluorinated

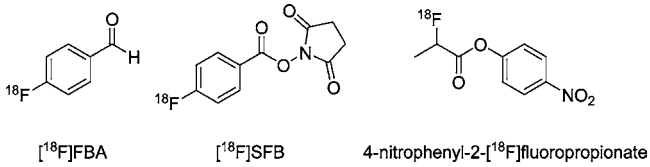


**FIGURE 10.** Prosthetic groups used for radiofluorination of RGD-analogues.

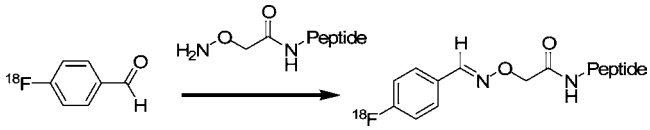


**FIGURE 11.** [18F]Labeling via oxime ligation.

via chemoselective one-step ligation of the aminooxy-functionalized peptide construct with 4-[18F]fluorobenzaldehyde via oxime formation (Figure 11).[21,58]

The affinity of *cyclo*(RGDfE)HEG-Dpr−[18F]FBOA vs (*cyclo*-(RGDfE)HEG)$_2$-K-Dpr−[18F]FBOA vs ((*cyclo*(RGDfE)HEG)$_2$-K)$_2$-K-Dpr-[18F]FBOA for the $\alpha_v\beta_3$-integrin increased by a factor of ~10 with each multimerization step (Figure 12), leading to improved tumor accumulation in the series tetramer > dimer > monomer (Figure 13).[21] Improvement in tracer stability was achieved by replacing the L-lysine tree used for multimerization by the corresponding D-lysine analogues.[59]

[18F]FB-E(*cyclo*(RGDyK))$_2$ and [18F]FB-E-[E(*cyclo*(RGDyK))$_2$]$_2$ were synthesized using a conventional 18F-acylation strategy.[60] Tumor uptake increased in the order tetramer > dimer > monomer; tumor/organ ratios, however, were substantially lower than those found for the [18F]FBOA multimers. In one study, kidney accumulation of [18F]FB-E(*cyclo*(RGDyK))$_2$ was significantly reduced by the introduction of a mini-PEG spacer between the prosthetic group and the peptide; tumor uptake remained unaffected.[61]

Recently, the E(*cyclo*(RGDyK))$_2$ analogue was radiofluorinated using click-chemistry.[62] This compound showed deteriorated pharmacokinetics compared with [18F]FB-E(*cyclo*-(RGDyK))$_2$ due to reduced tumor accumulation.

**Optical Probes.** Near infrared fluorescence (NIRF) optical imaging is gaining increasing importance as a powerful technology for the preclinical study of diseases at the molecular level or for intraoperative endoscopic fluorescence imaging. Blood and tissue absorbance as well as autofluorescence are

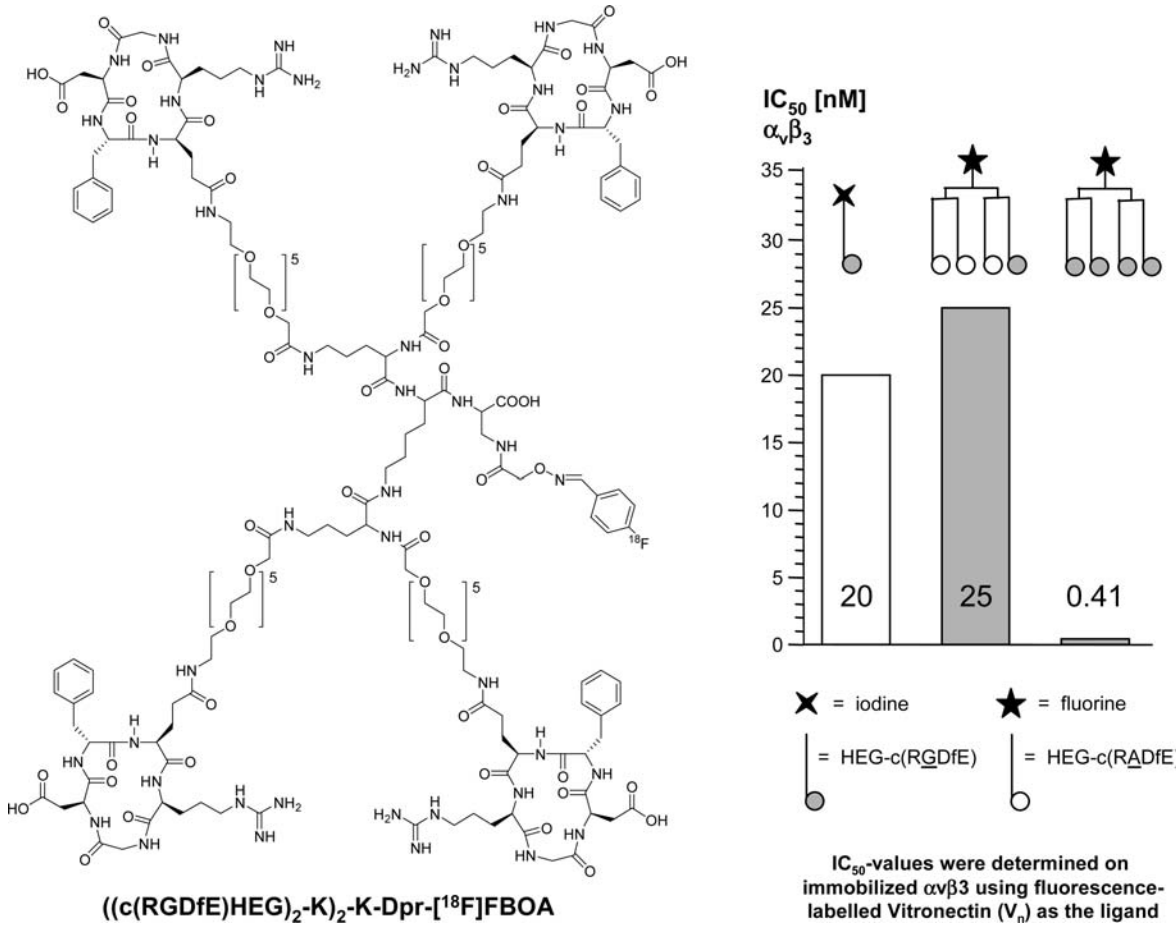


**FIGURE 12.** Structure of ((*cyclo*(RGDfE)HEG)$_2$-K)$_2$-K-Dpr−[18F]FBOA and its $\alpha_v\beta_3$-affinity compared with the respective monomeric analogue and a tetramer containing three knockout sequences (RADfE).

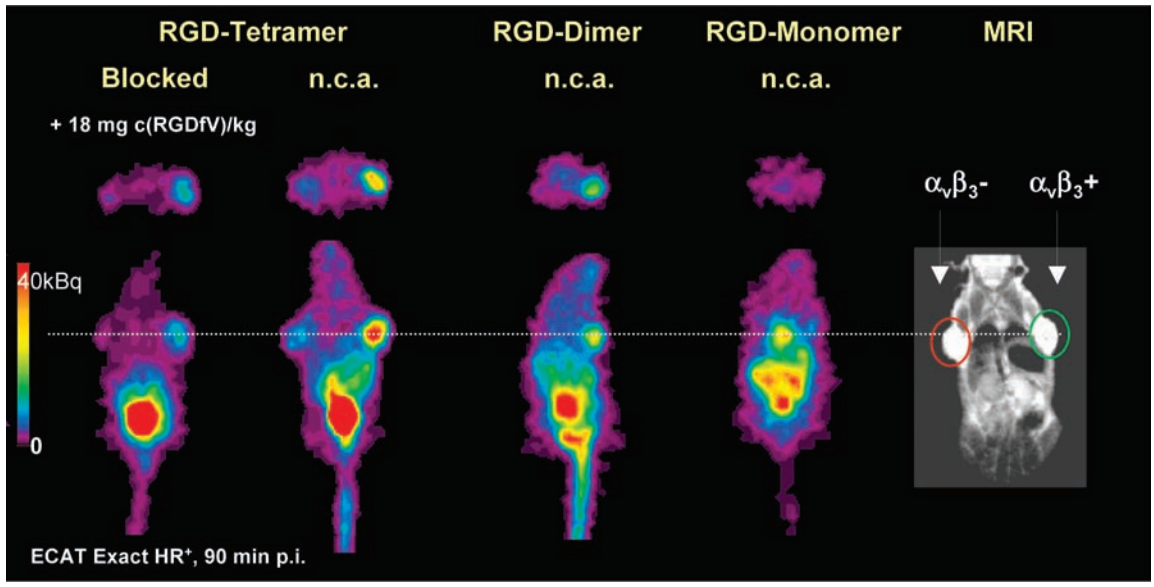


**FIGURE 13.** PET images of nude mice bearing M21 (high $\alpha_v\beta_3$-integrin expression) and M21L melanomas (low $\alpha_v\beta_3$-integrin expression) 90 min p.i. of (*cyclo*(RGDfE)HEG)$_2$-K)$_2$-K-Dpr-[$^{18}$F]FBOA and its dimeric and monomeric analogues.



minimal in the NIR window (650−900 nm), leading to efficient photon penetration into tissue (theoretical maximum, 7−14 cm) with low scattering.[63]

Both the availability of a variety of suitable NIR dyes, allowing easy coupling to targeting molecules,[64] and the development of fluorescence-mediated tomography (FMT), which is capable of resolving of fluorescence signatures quantitatively and three-dimensionally,[65] have prompted the development of several integrin-targeted NIR probes.

The first fluorescent $\alpha_v\beta_3$-integrin ligands applied for in vivo optical imaging were *cyclo*(RGDfK)−Cy5.5 and *cyclo*(RGDyK)−Cy5.5, both yielding high contrast images of mice bearing subcutaneous human xenografts.[66,67]

In the only FMT study performed so far, a disulfide bridged RGD peptide (*cyclo*[CRGDC]GK−Cy5.5) was used as the fluorescent probe, showing high and specific accumulation in M21 melanoma xenografts.[68]

Other fluorescent peptidic probes with selectivity for only the $\alpha_3$- or the $\beta_3$-integrin subunit, for example, have also been developed. The $\alpha_3$-binding analogues Cy5.5−OA02 (*cyclo*-(cGHCitGPQc)) and Cy5.5−LXY1 (*cyclo*(cdGLG-hydroxyproline-Nc)) show rapid washout from tumor, which can be circumvented by using a peptide−biotin−streptavidin−Cy5.5 construct with longer circulation time.[69,70] The fluorescent ligand Cyp-GRD (cypate-GRDSPK) lacks the RGD sequence but surprisingly shows highly specific uptake into $\alpha_v\beta_3$-integrin expressing tumors.[71] Experiments performed in $\beta_3$-knockout cells revealed that cellular uptake of Cyp-GRD was mediated exclusively by the $\beta_3$-subunit.[72]

A newly developed alternative to the use of dye-labeled ligands are semiconductor quantum dots (QDs).[29] QDs have excellent and tunable fluorescence characteristics and may easily be coated with targeting vectors such as small peptides and other functionalities. The use of QDs, either as a mono- (OI) or a dual-function probe (OI/PET), coated with up to 90 *c*(RGDyK) units per QD, has been reported recently[73,74] Despite excellent in vitro binding affinity, tumor accumulation of these probes was moderate, demonstrating limited extravasation of these nanoparticles. Consequently, QDs may allow exclusive targeting of vascular $\alpha_v\beta_3$-integrin expression.

**MR Probes.** Magnetic resonance imaging relies on the accelerated relaxation of the water protons in the surrounding tissue of a receptor ligand coupled with paramagnetic metals like $Gd^{3+}$. With an $\alpha_v\beta_3$-ligand, only the surrounding tissue of the integrin receptor will be detected, with a higher spatial resolution than that for nuclear imaging techniques.[75] For example, RGD-coated nanoparticles have already been applied for this new technique.[28] For a recent review about MRI, see ref 76.

## Clinical Experience

So far, successful transition into a clinical setting has only been achieved with radiolabeled $\alpha_v\beta_3$-targeted probes. Among these, [$^{18}$F]galacto-RGD, a glycosylated *cyclo*(RGDfK) analogue, was the first substance applied in patients, allowing imaging of $\alpha_v\beta_3$-expression in vivo with good tumor/background ratios due to its rapid renal excretion and

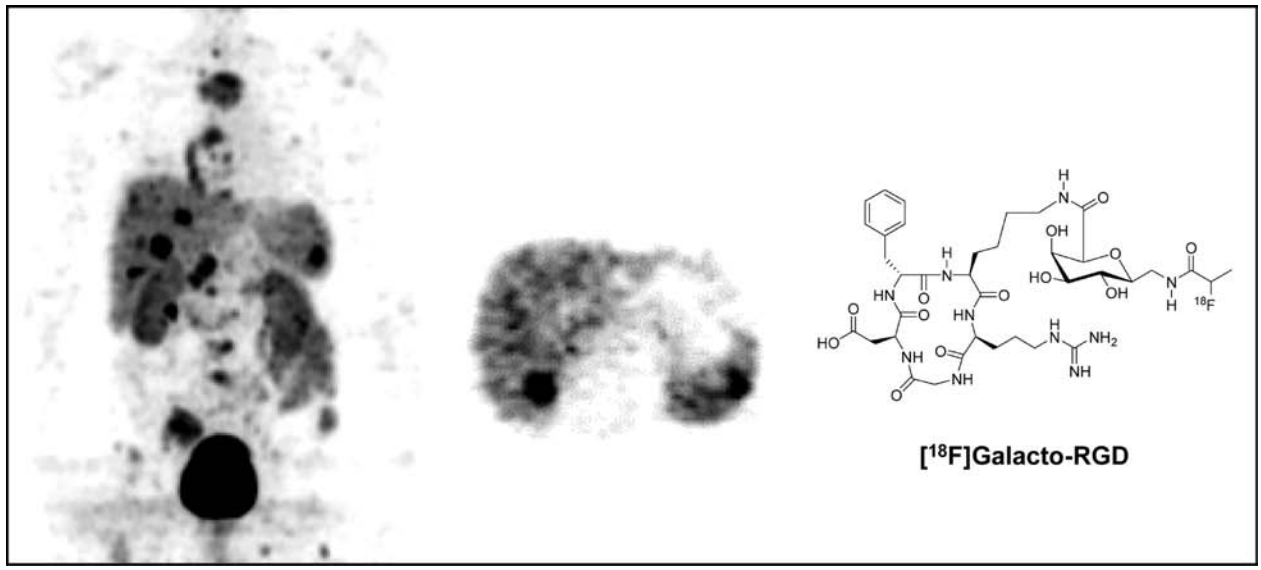


**FIGURE 14.** [$^{18}$F]Galacto-RGD PET of a patient with a bronchial carcinoid and multiple ossary, hepatic, and lienal metastases.

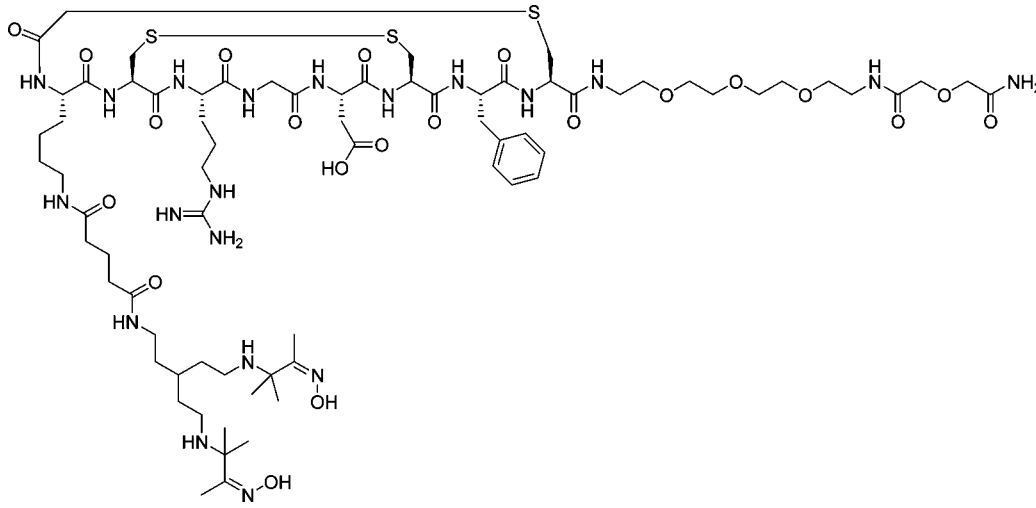

**FIGURE 15.** Structure of NC100692.[12]



inherently low background activity in most regions of the body.[77,78] The tumor uptake of [$^{18}$F]galacto-RGD correlates well with $\alpha_v\beta_3$-expression levels in tumors of various origin (Figure 14), as demonstrated by the correlation of tumor/blood ratios (calculated from standardized uptake values) with the immunohistochemical staining as well as microvessel density in excised tumor specimens.

Recently, another $^{18}$F-labeled RGD analogue was developed by Siemens and is now entering a clinical study.[79] Radiofluorination of $^{18}$F-RGD-K5 is performed using click chemistry. So far, no patient data on the performance of this tracer are available.

Furthermore, two compounds introduced by GE Healthcare have entered clinical studies, a $^{99m}$Tc-labeled RGD-containing compound, $^{99m}$Tc-NC100692 (Figure 15), and an $^{18}$F-labeled analog, $^{18}$F-AH111585, both sharing the same doubly cyclized peptide backbone based on RGD-4C and a PEGylated C-terminus. To allow labeling with $^{99m}$Tc and $^{18}$F, respectively, either a diamine−dioxime chelator or an aminooxy functionality were coupled to the Lys[1] side chain.

Both the SPECT and the PET tracer have so far been exclusively evaluated in breast cancer patients.[35,80] In patient images, both compounds show significantly higher background activity compared with [$^{18}$F]galacto-RGD, especially in liver. However, a more detailed assessment in a larger cohort of patients will be necessary for a valid comparison with the current "gold standard" [$^{18}$F]galacto-RGD.

## Conclusion

The data summarized in this Account indicate that quantification of integrin expression in vivo using powerful molecular

probes for tumor imaging and detection of neoangiogenesis is still an active field of research.

Future developments will aim toward the evaluation of the potential of other integrins, for example, the $\alpha_v\beta_6$-, $\alpha_4\beta_1$-, $\alpha_5\beta_1$-, and $\alpha_v\beta_5$-integrins, as potential targets for imaging angiogenic processes, not only in the context of tumor biology but also in other diseases such as myocardial infarction, stroke, atherosclerosis, peripheral artery disease, or chronic inflammation. It can be assumed that these efforts will possibly lead to valuable methods for monitoring of individualized therapies in the near future.

## BIOGRAPHICAL INFORMATION

**Margret Schottelius** obtained her diploma in Chemistry from the Eidgenössische Technische Hochschule Zurich, Switzerland, in 1997. In 2002, she received her Ph.D. in chemistry/radiopharmacy working with Prof. Hans-Jürgen Wester and Prof. Horst Kessler at the Technische Universität München (TUM). Her postdoctoral research focuses on the development and optimization of peptidic radiopharmaceuticals for cancer diagnosis and therapy.

**Burkhardt Laufer** earned his M.Sc. in Chemistry from the TUM in 2006. To date, he is pursuing his Ph.D. at the International Graduate School of Science and Engineering of the TUM under the supervision of Prof. Horst Kessler. His research focuses on synthesis of bioactive peptides and peptidomimetics.

**Horst Kessler** moved to the TUM as a full professor in 1988. Since 2008, he has been Carl von Linde Professor at the Institute for Advanced Study at the TUM, Department Chemie. His main interest is drug development from peptides and peptidomimetics, as well as the development and application of multidimensional NMR experiments to proteins, to small molecules, and to their interactions.

**Hans-Juergen Wester** is Professor of Radiopharmaceutical Chemistry at the TUM. He received his Ph.D. in Chemistry in 1995 from the University of Cologne. After a Postdoctoral Fellowship at the Department of Nuclear Medicine at the TUM, he became a faculty member in 2004. His interdisciplinary research focuses on the development of radiopharmaceuticals for positron emission tomography (PET) and single photon emission computed tomography (SPECT).

## FOOTNOTES

* To whom correspondence should be addressed. Mailing address: Klinikum rechts der Isar, Nuklearmedizinische Klinik und Poliklinik, Technische Universität München, Ismaninger Strasse 22, 81675 München, Germany. E-mail: h.j.wester@lrz.tum.de. Phone: +49 89 4140 2971. Fax: +49 89 4140 4841.

§ M.S. and B.L. contributed equally to this manuscript.

## REFERENCES

1 Folkman, J.; Klagsbrun, M. Angiogenic factors. *Science* **1987**, *235*, 442–447.

2 Risau, W. Mechanisms of angiogenesis. *Nature* **1997**, *386*, 671–674.

3 Hynes, R. O. A reevaluation of integrins as regulators of angiogenesis. *Nat. Med.* **2002**, *8*, 918–921.

4 Hynes, R. O. Integrins: Bidirectional, allosteric signaling machines. *Cell* **2002**, *110*, 673–687.

5 Haubner, R. Alpha(v)beta(3)-integrin imaging: A new approach to characterise angiogenesis? *Eur. J. Nucl. Med. Mol. Imaging* **2006**, *33* (1), 54–63.

6 Tamkun, J. W.; DeSimone, D. W.; Fonda, D.; Patel, R. S.; Buck, C.; Horwitz, A. F.; Hynes, R. O. Structure of integrin, a glycoprotein involved in the transmembrane linkage between fibronectin and actin. *Cell* **1986**, *46*, 271–282.

7 Humphries, M. J.; McEwan, P. A.; Barton, S. J.; Buckley, P. A.; Bella, J.; Mould, A. P. Integrin structure: Heady advances in ligand binding, but activation still makes the knees wobble. *Trends Biochem. Sci.* **2003**, *28*, 313–320.

8 Fox, J. E.; Shattil, S. J.; Kinlough-Rathbone, R. L.; Richardson, M.; Packham, M. A.; Sanan, D. A. The platelet cytoskeleton stabilizes the interaction between alpha(IIb)beta(3) and its ligand and induces selective movements of ligand-occupied integrin. *J. Biol. Chem.* **1996**, *271*, 7004–7011.

9 Pierschbacher, M. D.; Ruoslahti, E. Cell attachment activity of fibronectin can be duplicated by small synthetic fragments of the molecule. *Nature* **1984**, *309*, 30–33.

10 Meyer, A.; Auernheimer, J.; Modlinger, A.; Kessler, H. Targeting RGD recognizing integrins: Drug development, biomaterial research, tumor imaging and targeting. *Curr. Pharm. Des.* **2006**, *12*, 2723–2747.

11 Craig, W. S.; Cheng, S.; Mullen, D. G.; Blevitt, J.; Pierschbacher, M. D. Concept and progress in the development of RGD-containing peptide pharmaceuticals. *Biopolymers* **1995**, *37*, 157–175.

12 Edwards, D.; Jones, P.; Haramis, H.; Battle, M.; Lear, R.; Barnett, D. J.; Edwards, C.; Crawford, H.; Black, A.; Godden, V. 99mTc-NC100692-a tracer for imaging vitronectin receptors associated with angiogenesis: A preclinical investigation. *Nucl. Med. Biol.* **2008**, *35*, 365–375.

13 Gurrath, M.; Muller, G.; Kessler, H.; Aumailley, M.; Timpl, R. Conformation/activity studies of rationally designed potent anti-adhesive RGD peptides. *Eur. J. Biochem.* **1992**, *210*, 911–921.

14 Dechantsreiter, M. A.; Planker, E.; Mathä, B.; Lohof, E.; Hölzemann, G.; Jonczyk, A.; Goodman, S. L.; Kessler, H. N-Methylated cyclic RGD peptides as highly active and selective $\alpha_v\beta_3$ integrin antagonists. *J. Med. Chem.* **1999**, *42*, 3033–3040.

15 Haubner, R.; Wester, H. J.; Reuning, U.; Senekowitsch-Schmidtke, R.; Diefenbach, B.; Kessler, H.; Stocklin, G.; Schwaiger, M. Radiolabeled alpha(v)beta(3)-integrin antagonists: A new class of tracers for tumor targeting. *J. Nucl. Med.* **1999**, *40*, 1061–1071.

16 Haubner, R.; Gratias, R.; Diefenbach, B.; Goodman, S. L.; Jonczyk, A.; Kessler, H. Structural and functional aspects of RGD-containing cyclic pentapeptides as highly potent and selective integrin $\alpha_v\beta_3$ antagonists. *J. Am. Chem. Soc.* **1996**, *118*, 7461–7472.

17 Haubner, R.; Wester, H. J.; Burkhart, F.; Senekowitsch-Schmidtke, R.; Weber, W.; Goodman, S. L.; Kessler, H.; Schwaiger, M. Glycosylated RGD-containing peptides: Tracer for tumor targeting and angiogenesis imaging with improved biokinetics. *J. Nucl. Med.* **2001**, *42*, 326–336.

18 Haubner, R.; Wester, H. J.; Weber, W. A.; Mang, C.; Ziegler, S. I.; Goodman, S. L.; Senekowitsch-Schmidtke, R.; Kessler, H.; Schwaiger, M. Noninvasive imaging of alpha(v)beta(3)-integrin expression using 18F-labeled RGD-containing glycopeptide and positron emission tomography. *Cancer Res.* **2001**, *61*, 1781–1785.

19 Chen, X.; Hou, Y.; Tohme, M.; Park, R.; Khankaldyyan, V.; Gonzales-Gomez, I.; Bading, J. R.; Laug, W. E.; Conti, P. S. Pegylated Arg-Gly-Asp peptide: $^{64}$Cu-labeling and PET imaging of brain tumor alpha(v)beta(3)-integrin expression. *J. Nucl. Med.* **2004**, *45*, 1776–1783.

20 Chen, X.; Park, R.; Shahinian, A. H.; Bading, J. R.; Conti, P. S. Pharmacokinetics and tumor retention of $^{125}$I-labeled RGD peptide are improved by PEGylation. *Nucl. Med. Biol.* **2004**, *31*, 11–19.

21 Thumshirn, G.; Hersel, U.; Goodman, S. L.; Kessler, H. Multimeric cyclic RGD peptides as potential tools for tumor targeting: Solid-phase peptide synthesis and chemoselective oxime ligation. *Chemistry* **2003**, *9*, 2717–2725.

22 Sancey, L.; Ardisson, V.; Riou, L. M.; Ahmadi, M.; Marti-Batlle, D.; Boturyn, D.; Dumy, P.; Fagret, D.; Ghezzi, C.; Vuillez, J. P. In vivo imaging of tumour angiogenesis in mice with the alpha(v)beta(3)-integrin targeted tracer $^{99m}$Tc-RAFT-RGD. *Eur. J. Nucl. Med. Mol. Imaging* **2007**, *34*, 2037–2047.

23 Cai, W.; Wu, Y.; Chen, K.; Cao, Q.; Tice, D. A.; Chen, X. In vitro and in vivo characterization of $^{64}$Cu-labeled Abegrin, a humanized monoclonal antibody against integrin alpha(v)beta(3). *Cancer Res.* **2006**, *66*, 9673–9681.

24 Xiong, J. P.; Stehle, T.; Zhang, R.; Joachimiak, A.; Frech, M.; Goodman, S. L.; Arnaout, M. A. Crystal structure of the extracellular segment of integrin alpha(v)beta(3) in complex with an Arg-Gly-Asp ligand. *Science* **2002**, *296*, 151–155.

25 Marinelli, L.; Gottschalk, K. E.; Meyer, A.; Novellino, E.; Kessler, H. Human integrin $\alpha v\beta 5$: Homology modeling and ligand binding. *J. Med. Chem.* **2004**, *47*, 4166–4177.

26 Heckmann, D.; Meyer, A.; Laufer, B.; Zahn, G.; Stragies, R.; Kessler, H. Rational design of highly active and selective ligands for the alpha(5)beta(1)-integrin receptor. *ChemBioChem* **2008**, *9*, 1397–1407.

27 Harris, T. D.; Kalogeropoulos, S.; Nguyen, T.; Dwyer, G.; Edwards, D. S.; Liu, S.; Bartis, J.; Ellars, C.; Onthank, D.; Yalamanchili, P.; Heminway, S.; Robinson, S.; Lazewatsky, J.; Barrett, J. Structure−activity relationships of $^{111}$In- and $^{99m}$Tc-labeled quinolin-4-one peptidomimetics as ligands for the vitronectin receptor: Potential tumor imaging agents. *Bioconjugate Chem.* **2006**, *17*, 1294–1313.

28 Cai, W.; Chen, X. Multimodality molecular imaging of tumor angiogenesis. *J. Nucl. Med.* **2008**, *49* (2), 113S–128S.

29 Lieleg, O.; Lopez-Garcia, M.; Semmrich, C.; Auernheimer, J.; Kessler, H.; Bausch, A. R. Specific integrin labeling in living cells using functionalized nanocrystals. *Small* **2007**, *3*, 1560–1565.

30 Hughes, S.; Dobson, J.; El Haj, A. J. Magnetic targeting of mechanosensors in bone cells for tissue engineering applications. *J. Biomech.* **2007**, *40* (Suppl 1), S96–S104.

31 Xie, J.; Chen, K.; Lee, H. Y.; Xu, C.; Hsu, A. R.; Peng, S.; Chen, X.; Sun, S. Ultrasmall c(RGDyK)-coated $Fe_3O_4$ nanoparticles and their specific targeting to integrin $\alpha_v\beta_3$-rich tumor cells. *J. Am. Chem. Soc.* **2008**, *130*, 7542–7543.

32 Noiri, E.; Goligorsky, M. S.; Wang, G. J.; Wang, J.; Cabahug, C. J.; Sharma, S.; Rhodes, B. A.; Som, P. Biodistribution and clearance of $^{99m}$Tc-labeled Arg-Gly-Asp (RGD) peptide in rats with ischemic acute renal failure. *J. Am. Soc. Nephrol.* **1996**, *7*, 2682–2688.

33 Sivolapenko, G. B.; Skarlos, D.; Pectasides, D.; Stathopoulou, E.; Milonakis, A.; Sirmalis, G.; Stuttle, A.; Courtenay-Luck, N. S.; Konstantinides, K.; Epenetos, A. A. Imaging of metastatic melanoma utilising a technetium-99m labelled RGD-containing synthetic peptide. *Eur. J. Nucl. Med.* **1998**, *25*, 1383–1389.

34 Haubner, R.; Bruchertseifer, F.; Bock, M.; Kessler, H.; Schwaiger, M.; Wester, H. J. Synthesis and biological evaluation of a (99m)Tc-labelled cyclic RGD peptide for imaging the alpha(v)beta(3)-expression. *Nuklearmedizin* **2004**, *43*, 26–32.

35 Bach-Gansmo, T.; Danielsson, R.; Saracco, A.; Wilczek, B.; Bogsrud, T. V.; Fangberget, A.; Tangerud, A.; Tobin, D. Integrin receptor imaging of breast cancer: A proof-of-concept study to evaluate $^{99m}$Tc-NC100692. *J. Nucl. Med.* **2006**, *47*, 1434–1439.

36 Decristoforo, C.; Faintuch-Linkowski, B.; Rey, A.; von Guggenberg, E.; Rupprich, M.; Hernandez-Gonzales, I.; Rodrigo, T.; Haubner, R. [$^{99m}$Tc]HYNIC-RGD for imaging integrin alpha(v)beta(3)-expression. *Nucl. Med. Biol.* **2006**, *33*, 945–952.

37 Janssen, M. L.; Oyen, W. J.; Dijkgraaf, I.; Massuger, L. F.; Frielink, C.; Edwards, D. S.; Rajopadhye, M.; Boonstra, H.; Corstens, F. H.; Boerman, O. C. Tumor targeting with radiolabeled alpha(v)beta(3) integrin binding peptides in a nude mouse model. *Cancer Res.* **2002**, *62*, 6146–6151.

38 Liu, S.; Hsieh, W. Y.; Kim, Y. S.; Mohammed, S. I. Effect of coligands on biodistribution characteristics of ternary ligand $^{99m}$Tc-complexes of a HYNIC-conjugated cyclic RGDfK dimer. *Bioconjugate Chem.* **2005**, *16*, 1580–1588.

39 Liu, S.; He, Z.; Hsieh, W. Y.; Kim, Y. S.; Jiang, Y. Impact of PKM linkers on biodistribution characteristics of the $^{99m}$Tc-labeled cyclic RGDfK dimer. *Bioconjugate Chem.* **2006**, *17*, 1499–1507.

40 Liu, S.; Hsieh, W. Y.; Jiang, Y.; Kim, Y. S.; Sreerama, S. G.; Chen, X.; Jia, B.; Wang, F. Evaluation of a $^{99m}$Tc-labeled cyclic RGD tetramer for noninvasive imaging integrin $\alpha_v\beta_3$-positive breast cancer. *Bioconjugate Chem.* **2007**, *18*, 438–446.

41 Fani, M.; Psimadas, D.; Zikos, C.; Xanthopoulos, S.; Loudos, G. K.; Bouziotis, P.; Varvarigou, A. D. Comparative evaluation of linear and cyclic $^{99m}$Tc-RGD peptides for targeting of integrins in tumor angiogenesis. *Anticancer Res.* **2006**, *26*, 431–434.

42 Jung, K. H.; Lee, K. H.; Paik, J. Y.; Ko, B. H.; Bae, J. S.; Lee, B. C.; Sung, H. J.; Kim, D. H.; Choe, Y. S.; Chi, D. Y. Favorable biokinetic and tumor-targeting properties of $^{99m}$Tc-labeled glucosamino RGD and effect of paclitaxel therapy. *J. Nucl. Med.* **2006**, *47*, 2000–2007.

43 Decristoforo, C.; Santos, I.; Pietzsch, H. J.; Kuenstler, J. U.; Duatti, A.; Smith, C. J.; Rey, A.; Alberto, R.; Von Guggenberg, E.; Haubner, R. Comparison of in vitro and in vivo properties of [$^{99m}$Tc]cRGD peptides labeled using different novel Tc-cores. *Q. J. Nucl. Med. Mol. Imaging* **2007**, *51*, 33–41.

44 van Hagen, P. M.; Breeman, W. A.; Bernard, H. F.; Schaar, M.; Mooij, C. M.; Srinivasan, A.; Schmidt, M. A.; Krenning, E. P.; de Jong, M. Evaluation of a radiolabelled cyclic DTPA-RGD analogue for tumour imaging and radionuclide therapy. *Int. J. Cancer* **2000**, *90*, 186–198.

45 Dijkgraaf, I.; Kruijtzer, J. A.; Frielink, C.; Soede, A. C.; Hilbers, H. W.; Oyen, W. J.; Corstens, F. H.; Liskamp, R. M.; Boerman, O. C. Synthesis and biological evaluation of potent alpha(v)beta(3)-integrin receptor antagonists. *Nucl. Med. Biol.* **2006**, *33*, 953–961.

46 Decristoforo, C.; Hernandez Gonzalez, I.; Carlsen, J.; Rupprich, M.; Huisman, M.; Virgolini, I.; Wester, H. J.; Haubner, R. $^{68}$Ga- and $^{111}$In-labelled DOTA-RGD peptides for imaging of alpha(v)beta(3)-integrin expression. *Eur. J. Nucl. Med. Mol. Imaging* **2008**, *35*, 1507–1515.

47 Chen, X.; Liu, S.; Hou, Y.; Tohme, M.; Park, R.; Bading, J. R.; Conti, P. S. MicroPET imaging of breast cancer alphav-integrin expression with $^{64}$Cu-labeled dimeric RGD peptides. *Mol. Imaging Biol.* **2004**, *6*, 350–359.

48 Jia, B.; Liu, Z.; Shi, J.; Yu, Z.; Yang, Z.; Zhao, H.; He, Z.; Liu, S.; Wang, F. Linker effects on biological properties of $^{111}$In-labeled DTPA conjugates of a cyclic RGDfK dimer. *Bioconjugate Chem.* **2008**, *19*, 201–210.

49 Wu, Y.; Zhang, X.; Xiong, Z.; Cheng, Z.; Fisher, D. R.; Liu, S.; Gambhir, S. S.; Chen, X. microPET imaging of glioma integrin alpha(v)beta(3) expression using (64)Cu-labeled tetrameric RGD peptide. *J. Nucl. Med.* **2005**, *46*, 1707–1718.

50 Li, Z. B.; Cai, W.; Cao, Q.; Chen, K.; Wu, Z.; He, L.; Chen, X. (64)Cu-labeled tetrameric and octameric RGD peptides for small-animal PET of tumor alpha(v)beta(3)-integrin expression. *J. Nucl. Med.* **2007**, *48*, 1162–1171.

51 Dijkgraaf, I.; Kruijtzer, J. A.; Liu, S.; Soede, A. C.; Oyen, W. J.; Corstens, F. H.; Liskamp, R. M.; Boerman, O. C. Improved targeting of the alpha(v)beta(3)-integrin by multimerisation of RGD peptides. *Eur. J. Nucl. Med. Mol. Imaging* **2007**, *34*, 267–273.

52 Li, Z. B.; Chen, K.; Chen, X. (68)Ga-labeled multimeric RGD peptides for microPET imaging of integrin alpha(v)beta(3)-expression. *Eur. J. Nucl. Med. Mol. Imaging* **2008**, *35*, 1100–1108.

53 Sprague, J. E.; Kitaura, H.; Zou, W.; Ye, Y.; Achilefu, S.; Weilbaecher, K. N.; Teitelbaum, S. L.; Anderson, C. J. Noninvasive imaging of osteoclasts in parathyroid hormone-induced osteolysis using a $^{64}$Cu-labeled RGD peptide. *J. Nucl. Med.* **2007**, *48*, 311–318.

54 Jang, B. S.; Lim, E.; Hee Park, S.; Shin, I. S.; Danthi, S. N.; Hwang, I. S.; Le, N.; Yu, S.; Xie, J.; Li, K. C.; Carrasquillo, J. A.; Paik, C. H. Radiolabeled high affinity peptidomimetic antagonist selectively targets alpha(v)beta(3) receptor-positive tumor in mice. *Nucl. Med. Biol.* **2007**, *34*, 363–370.

55 Ogawa, M.; Hatano, K.; Oishi, S.; Kawasumi, Y.; Fujii, N.; Kawaguchi, M.; Doi, R.; Imamura, M.; Yamamoto, M.; Ajito, K.; Mukai, T.; Saji, H.; Ito, K. Direct electrophilic radiofluorination of a cyclic RGD peptide for in vivo alpha(v)beta(3)-integrin related tumor imaging. *Nucl. Med. Biol.* **2003**, *30*, 1–9.

56 Chen, X.; Park, R.; Shahinian, A. H.; Tohme, M.; Khankaldyyan, V.; Bozorgzadeh, M. H.; Bading, J. R.; Moats, R.; Laug, W. E.; Conti, P. S. $^{18}$F-labeled RGD peptide: Initial evaluation for imaging brain tumor angiogenesis. *Nucl. Med. Biol.* **2004**, *31*, 179–189.

57 Lee, Y. S.; Jeong, J. M.; Kim, H. W.; Chang, Y. S.; Kim, Y. J.; Hong, M. K.; Rai, G. B.; Chi, D. Y.; Kang, W. J.; Kang, J. H.; Lee, D. S.; Chung, J. K.; Lee, M. C.; Suh, Y. G. An improved method of $^{18}$F peptide labeling: Hydrazone formation with HYNIC-conjugated c(RGDyK). *Nucl. Med. Biol.* **2006**, *33*, 677–683.

58 Poethko, T.; Schottelius, M.; Thumshirn, G.; Hersel, U.; Herz, M.; Henriksen, G.; Kessler, H.; Schwaiger, M.; Wester, H. J. Two-step methodology for high-yield routine radiohalogenation of peptides: (18)F-labeled RGD and octreotide analogs. *J. Nucl. Med.* **2004**, *45*, 892–902.

59 Poethko, T.; Thumshirn, G.; et al. *J. Nucl. Med.* **2004**, *45*, 52P.

60 Wu, Z.; Li, Z. B.; Chen, K.; Cai, W.; He, L.; Chin, F. T.; Li, F.; Chen, X. microPET of tumor integrin alpha(v)beta(3)-expression using $^{18}$F-labeled PEGylated tetrameric RGD peptide ($^{18}$F-FPRGD4). *J. Nucl. Med.* **2007**, *48*, 1536–1544.

61 Wu, Z.; Li, Z. B.; Cai, W.; He, L.; Chin, F. T.; Li, F.; Chen, X. 18F-labeled mini-PEG spacered RGD dimer ($^{18}$F-FPRGD2): Synthesis and microPET imaging of alphavbeta3 integrin expression. *Eur. J. Nucl. Med. Mol. Imaging* **2007**, *34*, 1823–1831.

62 Li, Z. B.; Wu, Z.; Chen, K.; Chin, F. T.; Chen, X. Click chemistry for $^{18}$F-labeling of RGD peptides and microPET imaging of tumor integrin $\alpha_v\beta_3$ expression. *Bioconjugate Chem.* **2007**, *18*, 1987–1994.

63 Ntziachristos, V.; Ripoll, J.; Weissleder, R. Would near-infrared fluorescence signals propagate through large human organs for clinical studies? Errata. *Opt. Lett.* **2002**, *27*, 1652.

64 Tung, C. H. Fluorescent peptide probes for in vivo diagnostic imaging. *Biopolymers* **2004**, *76*, 391–403.

65 Ntziachristos, V.; Bremer, C.; Graves, E. E.; Ripoll, J.; Weissleder, R. In vivo tomographic imaging of near-infrared fluorescent probes. *Mol. Imaging* **2002**, *1*, 82–88.

66 Wang, W.; Ke, S.; Wu, Q.; Charnsangavej, C.; Gurfinkel, M.; Gelovani, J. G.; Abbruzzese, J. L.; Sevick-Muraca, E. M.; Li, C. Near-infrared optical imaging of integrin alpha(v)beta(3) in human tumor xenografts. *Mol. Imaging* **2004**, *3*, 343–351.

67 Chen, X.; Conti, P. S.; Moats, R. A. In vivo near-infrared fluorescence imaging of integrin alpha(v)beta(3) in brain tumor xenografts. *Cancer Res.* **2004**, *64*, 8009–8014.

68 von Wallbrunn, A.; Holtke, C.; Zuhlsdorf, M.; Heindel, W.; Schafers, M.; Bremer, C. In vivo imaging of integrin alpha(v)beta(3)-expression using fluorescence-mediated tomography. *Eur. J. Nucl. Med. Mol. Imaging* **2007**, *34*, 745–754.

69 Aina, O. H.; Marik, J.; Gandour-Edwards, R.; Lam, K. S. Near-infrared optical imaging of ovarian cancer xenografts with novel alpha(3)-integrin binding peptide "OA02". *Mol. Imaging* **2005**, *4*, 439–447.

70 Xiao, W.; Yao, N.; Peng, L.; Liu, R.; Lam, K. S. Near-infrared optical imaging in glioblastoma xenograft with ligand-targeting alpha(3)-integrin. *Eur. J. Nucl. Med. Mol. Imaging* **2009**, *36*, 94–103.

71 Achilefu, S.; Bloch, S.; Markiewicz, M. A.; Zhong, T.; Ye, Y.; Dorshow, R. B.; Chance, B.; Liang, K. Synergistic effects of light-emitting probes and peptides for targeting and monitoring integrin expression. *Proc. Natl. Acad. Sci. U.S.A.* **2005**, *102*, 7976–7681.

72 Bloch, S.; Xu, B.; Ye, Y.; Liang, K.; Nikiforovich, G. V.; Achilefu, S. Targeting beta(3)-integrin using a linear hexapeptide labeled with a near-infrared fluorescent molecular probe. *Mol. Pharmaceutics* **2006**, *3*, 539–549.

73 Cai, W.; Shin, D. W.; Chen, K.; Gheysens, O.; Cao, Q.; Wang, S. X.; Gambhir, S. S.; Chen, X. Peptide-labeled near-infrared quantum dots for imaging tumor vasculature in living subjects. *Nano Lett.* **2006**, *6*, 669–676.

74 Cai, W.; Chen, K.; Li, Z. B.; Gambhir, S. S.; Chen, X. Dual-function probe for PET and near-infrared fluorescence imaging of tumor vasculature. *J. Nucl. Med.* **2007**, *48*, 1862–1870.

75 Higuchi, T.; Wester, H. J.; Schwaiger, M. Imaging of angiogenesis in cardiology. *Eur. J. Nucl. Med. Mol. Imaging* **2007**, *34* (Suppl 1), S9–S19.

76 Cai, W.; Rao, J.; Gambhir, S. S.; Chen, X. How molecular imaging is speeding up antiangiogenic drug development. *Mol. Cancer Ther.* **2006**, *5*, 2624–2633.

77 Haubner, R.; Weber, W. A.; Beer, A. J.; Vabuliene, E.; Reim, D.; Sarbia, M.; Becker, K. F.; Goebel, M.; Hein, R.; Wester, H. J.; Kessler, H.; Schwaiger, M. Noninvasive visualization of the activated alpha(v)beta(3)-integrin in cancer patients by positron emission tomography and [$^{18}$F]Galacto-RGD. *PLoS Med.* **2005**, *2*, e70.

78 Beer, A. J.; Schwaiger, M. Imaging of integrin alpha(v)beta(3)-expression. *Cancer Metastasis Rev.* **2008**, *27*, 631–644.

79 Kolb, H. C.; Chen, K.; Walsh, J. C.; Gangadharmath, U.; Kasi, D.; Wang, B.; Duclos, B.; Liang, Q.; Padgett, H. C.; Karimi, F. USA, 2008.

80 Bach-Gansmo, T.; Bogsrud, T. V.; Skretting, A. Integrin scintimammography using a dedicated breast imaging, solid-state gamma-camera and (99m)Tc-labelled NC100692. *Clin. Physiol. Funct. Imaging* **2008**, *28*, 235–239.